





## Ultrafast PFAS degradation using oxidant-containing microdroplets

Cite this: *Chem. Commun.*, 2025, **61**, 17629

Received 8th July 2025,  
Accepted 26th September 2025

Yongqing Yang,<sup>a</sup> Md Tanim-Al Hassan,<sup>a</sup> Timothy Yaroshuk,<sup>a</sup> Juana Perez Sanchez,<sup>a</sup> Quentin A. Young,<sup>a</sup> Richard N. Zare <sup>b</sup> and Hao Chen <sup>\*a</sup>

DOI: 10.1039/d5cc03862f

rsc.li/chemcomm

**Toxic PFASs usually require a long time and a high energy input for effective degradation. This study reports an ultrafast and effective method for degrading PFASs using microdroplets containing persulfate or Fenton's reagent. A 77–94% degradation efficiency was obtained for perfluorocarboxylic acids (PFCAs) in <1 ms under ambient conditions.**

As per- and poly-fluoroalkyl substances (PFASs) present a threat to human health,<sup>1</sup> the development of strategies for the effective degradation of PFASs is of paramount importance. The common methods for PFAS degradation include advanced oxidation,<sup>2</sup> electrochemical oxidation,<sup>3</sup> photodegradation,<sup>4</sup> biodegradation,<sup>5</sup> irradiation,<sup>6</sup> plasma degradation,<sup>7</sup> and thermal degradation.<sup>8</sup> However, the majority of these methods require precise control of the reaction conditions, extended reaction times, and high energy input to achieve high degradation efficiency. A significant focus has been placed on enhancing the degradation efficiency through the incorporation of additives. Commonly employed additives include hydrogen peroxide and persulfate ( $S_2O_8^{2-}$ ), as they are capable of decomposing into highly reactive hydroxyl radicals ( $\bullet OH$ ) and sulfate radicals ( $SO_4^{\bullet -}$ ), respectively. These reactive species,  $\bullet OH$  and  $SO_4^{\bullet -}$ , exhibit strong oxidative potentials (2.8 V vs. SHE for  $\bullet OH$ , 2.5–3.1 V vs. SHE for  $SO_4^{\bullet -}$ ),<sup>9</sup> enabling them to effectively break down persistent organic pollutants.<sup>10,11</sup> However, for PFAS degradation in bulk solution, these two additives do not perform well.<sup>12</sup>

Currently, the microdroplet method has garnered increasing attention due to its capability to significantly accelerate a wide range of chemical reactions.<sup>13–17</sup> However, the application of a microdroplet-based method for PFAS degradation remains relatively underexplored.<sup>18,19</sup> Although a previous study<sup>18</sup> in this area has reported relatively low degradation efficiencies and challenges in achieving rapid and highly effective

degradation, the inherent advantages of microdroplet systems warrant further investigation. In this study, we employed Fenton's reagent ( $H_2O_2/Fe^{2+}$ ) and persulfate ( $S_2O_8^{2-}$ ) as oxidant additives in conjunction with microdroplet reactions to degrade PFASs. Our findings demonstrated that both additives achieved highly efficient degradation of 10  $\mu M$  perfluorooctanoic acid (PFOA, >90% degradation efficiencies) in less than 1 millisecond. Furthermore, we observed that this method is particularly effective for degrading short-chain PFCAs, such as PFHpA, PFHxA, and PFPeA, which are typically more resistant to degradation. For perfluorooctane sulfonic acid (PFOS,  $C_8F_{17}SO_3H$ ), which is reported to be hardly degraded in microdroplets,<sup>18</sup> adding additives led to over 50% degradation efficiency. This highlights the robust degradation capability of our approach, underscoring its potential as a rapid and efficient strategy for PFAS remediation.

In our experiment, for the microdroplet reaction, we used the setup shown in Fig. 1a. Briefly, a syringe pump was used to introduce 300  $\mu L$  of sample solution (10  $\mu M$  PFAS, 5%  $H_2O_2$ , and 0.1 mM  $FeCl_2$ , or 10  $\mu M$  PFAS and 5 mM  $Na_2S_2O_8$ ) into a home-built sonic spray ionization (SSI)<sup>20</sup> sprayer *via* a piece of capillary at a flow rate of 10  $\mu L \text{ min}^{-1}$ . The sprayed microdroplets were collected using an Eppendorf vial and the collected sample was reconstituted to 300  $\mu L$  prior to LC/MS analysis. As a control, the same sample solution was shaken in a vial for 30 min for comparison and examined by LC/MS.

In this study, the degradation efficiency of PFOA ( $C_7F_{15}COOH$ ) without any oxidant additives under microdroplet conditions (PFOA-MD) was experimentally investigated first and the results are presented in Fig. S1. The degradation efficiency of PFOA was calculated using the following formula:

$$\text{Degradation efficiency} = (P_1 - P_2)/P_1 \quad (1)$$

where  $P_1$  represents the extracted ion chromatogram (EIC) peak area for the 10  $\mu M$  PFOA solution before the reaction, and  $P_2$  represents the EIC peak area of the sample after the reaction. All subsequent degradation efficiency calculations were performed in the same way. As shown in Fig. S1a and b, the EIC

<sup>a</sup> Department of Chemistry & Environmental Science, New Jersey Institute of Technology, Newark, NJ, USA. E-mail: hao.chen.2@njit.edu

<sup>b</sup> Department of Chemistry, Stanford University, Stanford, California 94305-5080, USA



**Fig. 1** (a) Schematic diagram showing our microdroplet setup. EIC of the signal  $[\text{PFPeA-H}]^-$  of 10  $\mu\text{M}$  PFPeA (b) before degradation and (c) after degradation in microdroplets without oxidant, (d) after degradation in bulk solution using  $\text{S}_2\text{O}_8^{2-}$  additive, (e) after degradation in microdroplets containing  $\text{S}_2\text{O}_8^{2-}$  additive, (f) after degradation in bulk solution using Fenton's reagent additive, and (g) after degradation in microdroplets containing Fenton's reagent.

peak area of intact  $[\text{PFOA-H}]^-$  ion was  $1.14 \times 10^8$  and  $9.30 \times 10^7$  before and after degradation using microdroplets without adding any additives, showing an 18% degradation efficiency that is consistent with previously reported results using microdroplet technology for PFOA degradation.<sup>18</sup> The concentration of fluoride ions generated after degradation was also measured to be 2.1  $\mu\text{M}$  using a fluoride meter (Life Technologies, Chicago, IL, USA, see detailed  $\text{F}^-$  measurement procedure in the SI), corresponding to 7.7% of fluorine being converted into  $\text{F}^-$  (Table S1). The latter is calculated using the equation:

$$\text{Percentage of fluorine converted into } \text{F}^- = 2.1 \mu\text{M} / (10 \mu\text{M} \times m \times \text{DE}) \times 100\% \quad (2)$$

where 10  $\mu\text{M}$  is the initial concentration of PFOA,  $m$  is the number of fluorine atoms per PFOA molecule, and DE is the degradation efficiency. Subsequently, an analysis of potential short-chain PFAS products generated from PFOA degradation was conducted. No short-chain PFAS products were detected in the LC/MS analysis, which is consistent with previous studies.<sup>18</sup> This result of 7.7% fluorine conversion into fluorides indicates that some fluorines from the degraded PFOA may be contained in some volatile degradation products that were not collected or in some forms that were not well detected by LC/MS.

Subsequently, the degradation efficiencies of PFOA using  $\text{S}_2\text{O}_8^{2-}$  as an additive under both bulk and microdroplet conditions were compared, and the results are presented in Fig. S1 and Table S1. As shown in Fig. S1c, while  $\text{S}_2\text{O}_8^{2-}$  can slightly facilitate PFOA degradation under bulk conditions, the efficiency was relatively low, reaching only 8.77% (the EIC peak areas of 10  $\mu\text{M}$  PFOA before and after bulk digestion are  $1.14 \times 10^8$  and  $1.04 \times 10^8$ , respectively). This is lower than the degradation efficiency of 18% achieved under microdroplet conditions, as mentioned above (PFOA-MD, Fig. S1b), indicating

that the degradation rate of PFOA by  $\text{S}_2\text{O}_8^{2-}$  in bulk solution is comparatively slow. In stark contrast, under microdroplet conditions with  $\text{S}_2\text{O}_8^{2-}$  as the additive (Fig. S1d), a degradation efficiency of 90.0% was achieved, representing a significant enhancement compared to the bulk condition with persulfate or microdroplet condition without using persulfate. The degradation efficiency was further confirmed by using calibration curve measurements (Fig. S2 and S3, see discussion in SI). This indicates that the combination of microdroplets and  $\text{S}_2\text{O}_8^{2-}$  can greatly activate PFOA, thereby enabling highly efficient degradation. Finally, the fluoride ion concentration in the degradation products of  $\text{S}_2\text{O}_8^{2-}$  as an additive under both methods was measured and the results are presented in Table S1. It can be observed that the microdroplet method not only exhibits higher degradation efficiency but also achieves significantly greater fluoride ion conversion (25.8%, Table S1) compared to the bulk method (2.2%). The distance between the sprayer and the quenching solution in the vial was 2 cm, and the speed of the sprayed microdroplets was  $84 \pm 18 \text{ m s}^{-1}$  as previously measured.<sup>21</sup> Thus, the flight time of the microdroplet between the sprayer and the quenching solution was only 250  $\mu\text{s}$  [ $2 \text{ cm} / (84 \text{ m s}^{-1}) \cong 250 \mu\text{s}$ ], which is significantly shorter than the 30 min used under bulk conditions (differing by a factor of about 2 million). Despite this drastic reduction in reaction time, the degradation efficiency of the microdroplet method is markedly higher, with the degradation rate enhanced by over a factor of 2 million.

Fig. S1e and f present the results of PFOA degradation using Fenton's reagent as an additive. Under the bulk condition, the degradation efficiency was only 3.1% (Fig. S1e), which is significantly lower than the 92.7% achieved under microdroplet conditions (Fig. S1f). This further demonstrates the power of the microdroplet technique. Furthermore, by comparing the fluoride ion concentration in the degradation products, it is observed that the fluoride ion conversion rate for both conditions was approximately 7%, which is only about one-quarter of that achieved when  $\text{S}_2\text{O}_8^{2-}$  was used as the additive (Table S1). This suggests that the primary degradation mechanisms of the two additives are different, as discussed below. Again, LC/MS analysis of the degradation products from both additives revealed no presence of shorter-chain PFOA products. These results emphasize the effectiveness of using the microdroplet technique combined with an oxidant for PFOA degradation.

Previous studies have extensively investigated the degradation of PFASs;<sup>22</sup> however, research on the degradation of short-chain PFASs (with 4–7 carbon atoms) remains limited. Short-chain PFASs have gained increasing attention due to their potential use as substitutes for long-chain PFAS compounds and their higher mobility in aquatic environments.<sup>23</sup> This study evaluated the degradation efficiency of short-chain PFCAs, such as PFHpA ( $\text{C}_6\text{F}_{13}\text{COOH}$ ), PFHxA ( $\text{C}_5\text{F}_{11}\text{COOH}$ ), and PFPeA ( $\text{C}_4\text{F}_9\text{COOH}$ ), under oxidant-containing microdroplet conditions. Using PFPeA as an example, Fig. 1b shows the EIC peak of undegraded 10  $\mu\text{M}$  PFPeA. As shown in Fig. 1c, in the absence of any additive, the microdroplet method alone achieved a degradation efficiency of only 9.8%, which is half of that observed

for PFOA under the same conditions as mentioned before. This finding confirms that PFPeA is indeed more challenging to degrade. When  $S_2O_8^{2-}$  was used as an additive, the degradation efficiency in bulk conditions was merely 6.5% (Fig. 1d), whereas, under microdroplet conditions, it increased significantly to 80.8% (Fig. 1e). Similarly, when Fenton's reagent was employed as an additive, the degradation efficiency in bulk conditions (Fig. 1f) remained low (5.1%), while in microdroplet conditions, it reached 77.6% (Fig. 1g). These results indicate that the microdroplets facilitate the degradation of PFPeA effectively.

For PFHpA and PFHxA, similarly, the degradation efficiency using the microdroplet method without any additive remained low (17.1% for PFHpA and 16.8% for PFHxA), as shown in Fig. S4a, b and S5a, b. Analysis of Fig. S4c–f and S5c–f further reveals that their degradation efficiencies remained low (below 6%) under bulk conditions using the two oxidant additives. However, when the microdroplet method with oxidants was applied, their degradation efficiencies approached 90%. Again, in the case of PFHpA and PFHxA as well as PFPeA, a higher percentage of the fluorine content was converted into fluoride ions (*ca.* 20%, Table S2) when  $S_2O_8^{2-}$  was used under microdroplet conditions. In contrast, when Fenton's reagent was used as the additive, a lower fluoride conversion rate was observed (*ca.* 10%, Table S2).

Fig. S6 summarizes the degradation efficiencies for PFCAs of different chain lengths under various conditions. For all the tested PFCAs, the degradation efficiencies under bulk conditions are consistently lower than those achieved using the microdroplet method. Moreover, in the presence of additives in the microdroplets, the degradation efficiencies are significantly enhanced. These findings demonstrate that the oxidant-containing microdroplet method not only accelerates the degradation rate of PFCAs, but also improves the degradation efficiency for PFCAs with different chain lengths. Previous studies have shown that PFOA and PFOS do not degrade in the presence of hydroxyl radicals in bulk solutions, even under Fenton reaction conditions.<sup>24,25</sup> However, our results demonstrate that both  $\bullet OH$  and  $SO_4^{\bullet -}$  radicals can degrade PFAS in microdroplets, indicating that our method effectively enhances the oxidative power of these radicals. Additionally, for radical activation, researchers have commonly employed UV light to activate  $\bullet OH$  radicals or adjusted the pH to influence the degradation efficiency of the radicals.<sup>26,27</sup> However, in our microdroplet-based method, no additional activation is required, which represents a significant advantage.

One limitation of our microdroplet method applied in this study is the small PFAS sample volume used, which currently hinders its direct application in industrial settings. However, recently, several new microdroplet generation systems have been developed to scale up microdroplet-based reactions. For example, Liu *et al.*<sup>28</sup> designed a large-scale industrial microdroplet reactor for  $CO_2$  utilization, and Xu *et al.*<sup>29</sup> developed a Swirl-Venturi microdroplet generator capable of producing small droplets with high throughput. These advancements indicate that our method has strong potential for industrial application in large-scale PFAS treatment by integrating it with emerging scalable microdroplet technologies.

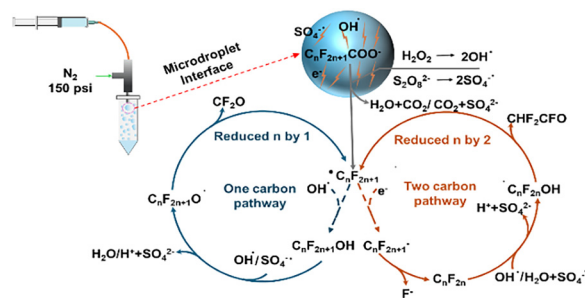


Fig. 2 Proposed degradation pathways of PFCAs on aqueous droplet surfaces.

We further proposed a mechanism for the PFCAs degradation under oxidant-containing microdroplet conditions, as illustrated in Fig. 2. In the microdroplet environment, PFCAs undergo electro-spray ionization, forming negatively charged  $C_nF_{2n+1}COO^-$  ions. These ions are subsequently attacked by hydroxyl radicals ( $\bullet OH$ ) or sulfate radicals ( $SO_4^{\bullet -}$ ) generated from the oxidants,<sup>11</sup> leading to the formation of  $C_nF_{2n+1}\bullet$  radicals and  $H_2O + CO_2$  (or  $CO_2 + SO_4^{2-}$ ). The subsequent degradation follows two possible pathways as proposed previously:<sup>18</sup> a one-carbon degradation pathway or a two-carbon degradation pathway.

The one-carbon degradation pathway involves the reaction of  $C_nF_{2n+1}\bullet$  radicals with  $\bullet OH$  to form  $C_nF_{2n+1}OH$ . Subsequently,  $\bullet OH$  or  $SO_4^{\bullet -}$  reacts with  $C_nF_{2n+1}OH$  to generate  $C_nF_{2n+1}O\bullet$ .  $C_nF_{2n+1}O\bullet$  readily loses  $CF_2O$ , forming  $C_{n-1}F_{2n-1}\bullet$ , which then enters the next degradation cycle. In this case,  $CF_2O$  is a colorless gas and difficult to ionize, accounting for the reason that it was not detected by LC/MS. For the two-carbon degradation pathway, the process begins with  $C_nF_{2n+1}\bullet$  undergoing electron attack (presumably present in microdroplets) to form the negatively charged  $C_nF_{2n+1}^-$  ion. This ion readily loses  $F^-$ , generating the neutral species  $C_nF_{2n}$  that cannot be detected by LC/MS. The  $\bullet OH$  or  $SO_4^{\bullet -}$  then attacks  $C_nF_{2n}$ , forming the radical intermediate  $\bullet C_nF_{2n}OH$ . Due to the instability of the  $\bullet C_nF_{2n}OH$  structure, it readily loses  $CHF_2CFO$  (as a result, the fluorine conversion efficiency to fluoride in this pathway is 25%), resulting in the removal of two carbon atoms and forming  $C_{n-2}F_{2n-3}\bullet$ , which then enters the next degradation cycle.

Both the oxidant additives and microdroplets can facilitate the two degradation pathways. On the one hand, the oxidant provides  $\bullet OH$  or  $SO_4^{\bullet -}$  to attack PFAS, promoting the conversion of  $C_nF_{2n+1}\bullet$  into  $C_nF_{2n+1}OH$  and thereby facilitating the one-carbon degradation pathway. On the other hand, the microdroplet environment could enhance surface contact and mass transfer, further accelerating the overall degradation process. The detection of fluoride ions in the degradation products under microdroplet conditions for both additives suggests the occurrence of the two-carbon degradation pathway, as this is the pathway that releases free fluoride ions (the fluorine conversion efficiency to fluoride is 25% since the other product is the volatile  $CHF_2CFO$ , Fig. 2). However, the significant difference in fluoride ion conversion efficiencies between the two additives suggests that they favor different



Fig. 3 EIC of the signal  $[\text{PFOS-H}]^-$  of  $10 \mu\text{M}$  PFOS (a) before degradation, (b) after degradation in microdroplets without oxidant additive, (c) after degradation in bulk solution using  $\text{S}_2\text{O}_8^{2-}$  additive, (d) after degradation in microdroplets containing  $\text{S}_2\text{O}_8^{2-}$ , (e) after degradation in bulk solution using Fenton's reagent additive, and (f) after degradation in microdroplets containing Fenton's reagent.

primary degradation pathways. For microdroplet degradation using  $\text{S}_2\text{O}_8^{2-}$ , the fluoride ion conversion efficiency was approximately 20%. It can be inferred that 80% of the degradation under this condition occurs *via* the two-carbon pathway ( $80\% \times 25\% = 20\%$ ), while the remaining 20% proceeds through the one-carbon pathway. For microdroplet degradation using Fenton's reagent, the fluoride ion conversion efficiency was generally below 10%, indicating that less than 40% of fluorine atoms undergo degradation *via* the two-carbon pathway ( $40\% \times 25\% = 10\%$ ), with the majority ( $>60\%$ ) following the one-carbon pathway. This is consistent with the one-carbon degradation mechanism, as the abundant  $\bullet\text{OH}$  radicals generated by Fenton's reagent promote the conversion of  $\text{C}_n\text{F}_{2n+1}\bullet$  into  $\text{C}_n\text{F}_{2n+1}\text{OH}$ , thereby driving the one-carbon degradation process (Fig. 2).

Perfluorosulfonic acids (PFSAs) have been previously reported to be resistant to degradation in microdroplets.<sup>18</sup> Therefore, this study investigated whether the addition of oxidant additives enables the efficient degradation of PFOS, a representative PFSA compound, under microdroplet conditions. First, we observed no degradation using microdroplets only (Fig. 3b), which is consistent with the previous study.<sup>18</sup> Next, we examined the catalytic degradation efficiency of PFOS in the presence of the two additives, and the results are presented in Fig. 3. Under bulk conditions, the PFOS degradation efficiency remained below 4% with both additives (Fig. 3c and e), indicating negligible degradation. However, under microdroplet conditions, the degradation efficiency increased to 53.9% with  $\text{S}_2\text{O}_8^{2-}$  (Fig. 3d) as the additive and 63.1% with Fenton's reagent (Fig. 3f). Although these values are lower than the degradation efficiencies observed for PFCAs under the same conditions, they are significantly higher than those achieved with either the microdroplet method alone or bulk-phase additive degradation. This result further confirms that the microdroplet technique can effectively catalyze reactions that are otherwise difficult to achieve under bulk conditions.

This study demonstrates, for the first time, the effective degradation of PFAS using microdroplets containing  $\text{S}_2\text{O}_8^{2-}$  or Fenton's reagent. Under bulk conditions, these additives

achieved minimal degradation ( $<9\%$  for PFOA within 30 min). However, in the microdroplet environment, the PFOA degradation efficiency increased to 18% without additives and reached  $\sim 90\%$  when additives were introduced, with a reaction time of less than 1 millisecond. Similar trends were observed for short-chain PFCAs (PFHpA, PFHxA, PFPeA), where the degradation efficiencies exceeded 80% with additives under microdroplet conditions. Product analysis suggests that PFCA degradation possibly follows one-carbon and two-carbon degradation mechanisms. In addition, PFOS, previously considered resistant to microdroplet degradation, exhibited nearly 60% degradation within 1 ms when additives were introduced. These findings highlight the strong catalytic effect of oxidant-containing microdroplets for rapid PFAS degradation, offering valuable insights for the development of efficient PFAS remediation strategies in both academic and industrial applications.

YY, RNZ and HC designed the research; YY, MTAH, TY, JPS, and QAY performed the research. We thank NSF (CHE-2505727) for supporting this work.

## Conflicts of interest

The authors declare no competing financial interest.

## Data availability

The supplementary data have been included as part of the supplementary information (SI). Supplementary information: experimental details and additional data. See DOI: <https://doi.org/10.1039/d5cc03862f>.

## Notes and references

- 1 K. Steenland and A. Winquist, *Environ. Res.*, 2021, **194**, 110690.
- 2 M. Gar Alalm and D. C. Boffito, *Chem. Eng. J.*, 2022, **450**, 138352.
- 3 N. Kim, *et al.*, *Nat. Commun.*, 2024, **15**, 8321.
- 4 H. Zhang, *et al.*, *Nature*, 2024, **635**, 610–617.
- 5 J. Li, *et al.*, *Nat. Commun.*, 2022, **13**, 4368.
- 6 D. Patch, *et al.*, *Sci. Total Environ.*, 2022, **832**, 154941.
- 7 R. K. Singh, *et al.*, *Environ. Sci. Technol.*, 2019, **53**, 2731–2738.
- 8 R. Sun, *et al.*, *Environ. Sci. Technol.*, 2024, **58**, 22417–22430.
- 9 S. Guerra-Rodríguez, *et al.*, *Water*, 2018, **10**, 1828.
- 10 X. Lu, *et al.*, *J. Hazard. Mater.*, 2021, **403**, 123915.
- 11 X. Guo, *et al.*, *Appl. Catal. B*, 2025, **371**, 125214.
- 12 J. Bannister, PhD, Luleå University of Technology, 2020.
- 13 X. Yan, *et al.*, *Angew. Chem., Int. Ed.*, 2016, **55**, 12960–12972.
- 14 X. Yan, *et al.*, *Angew. Chem., Int. Ed.*, 2017, **56**, 3562–3565.
- 15 M. Girod, *et al.*, *Angew. Chem., Int. Ed.*, 2024, **63**, e202400118.
- 16 L. Qiu and R. G. Cooks, *Angew. Chem., Int. Ed.*, 2024, **63**, e202400118.
- 17 C. Liu, *et al.*, *Chem. Sci.*, 2019, **10**, 9367–9373.
- 18 D. Xia, *et al.*, *J. Am. Chem. Soc.*, 2024, 11266–11271.
- 19 K. Li, *et al.*, *Environ. Sci. Technol.*, 2023, **57**, 21448–21458.
- 20 Z. Takáts, *et al.*, *Anal. Chem.*, 2004, **76**, 4050–4058.
- 21 J. K. Lee, *et al.*, *Proc. Natl. Acad. Sci. U. S. A.*, 2015, **112**, 3898–3903.
- 22 S. C. E. Leung, *et al.*, *Sci. Total Environ.*, 2022, **827**, 153669.
- 23 E. Gagliano, *et al.*, *Water Res.*, 2020, **171**, 115381.
- 24 A. Santos, *et al.*, *Sci. Total Environ.*, 2016, **563–564**, 657–663.
- 25 H. Hori, *et al.*, *Environ. Sci. Technol.*, 2004, **38**, 6118–6124.
- 26 H. Javed, *et al.*, *Chemosphere*, 2020, **247**, 125883.
- 27 Y. Lai, *et al.*, *Chemosphere*, 2024, **357**, 141951.
- 28 X. Liu, *et al.*, *J. Am. Chem. Soc.*, 2025, **147**, 3529–3538.
- 29 Y. Xu, *et al.*, *Ind. Eng. Chem. Res.*, 2024, **63**, 8416–8429.